

1994 NASA/ASEE SUMMER FACULTY FELLOWSHIP PROGRAM 111753

S2-18

JOHN F. KENNEDY SPACE CENTER
UNIVERSITY OF CENTRAL FLORIDA

33962

P. 30

SPACE STATION RACKS WEIGHT & C.G. MEASUREMENT
USING THE RACK INSERTION END-EFFECTOR

| | |
|----------------------------|--|
| PREPARED BY: | Dr. William V. Brewer |
| ACADEMIC RANK: | Professor |
| UNIVERSITY AND DEPARTMENT: | Jackson State University Technology Department |
| NASA/KSC | |
| DIVISION: | Mechanical Engineering |
| BRANCH: | Special Projects |
| NASA COLLEAGUE: | Eduardo Lopez Alan Littlefield |
| DATE: | August 1, 1994 |
| CONTRACT NUMBER: | University of Central Florida NASA-NGT-60002 Supplement: 17 |

ACKNOWLEDGEMENTS

Eduardo Lopez provided a good work environment upon arrival here at the robotics lab. He framed the problem well and got the project off to a good start. Alan Littlefield shared time and information to keep the effort focused on the customers perspective. N.S.Malladi offered advice, alternatives and assistance whenever asked. Carey Cooper vastly improved the graphics of this presentation by making the relevant computer drawings available in a usable form. He also shared his experience regarding strut linkage attachment hardware. My appreciation goes to these and many others who made the work here a pleasure. My thanks to Loren Anderson and Kari Styles for putting up with us and answering all the same questions over and over. It's been fun guys and I hope we can do it again.

ABSTRACT

Objective: Design a method to measure weight and center of gravity (C.G.) location for Space Station Modules by adding sensors to the existing Rack Insertion End Effector (RIEE).
Accomplishments: Alternative sensor placement schemes are organized into categories. Vendors were queried for suitable sensor equipment recommendations. Inverse mathematical models for each category determine expected maximum sensor loads. Sensors are selected using these computations, yielding cost and accuracy data. Accuracy data for individual sensors are inserted into forward mathematical models to estimate the accuracy of an overall sensor scheme. Cost of the schemes can be estimated. Ease of implementation and operation are discussed.

SUMMARY

Scope: Non-experimental assessment of competing sensor placement schemes to determine accuracy, cost, installation and operational characteristics of selected alternatives.

Range of variables: Measured weight within $\pm 0.2\%$ of actual weight
" C.G. " " 0.4 in. of " C.G.

Constraints:

| | |
|----------------|--|
| Rack weight: | $250 < W_r < 1750$ lbs. |
| C.G. envelope: | 6.3 x 4.6 x 11.4 ins. |
| Sensor ranges: | 500, 1000, 2000 lbs. (off-the-shelf) |
| " accuracies: | 0.05 % of full scale (" " "maximum) |

Results: Selected sensor schemes are evaluated for accuracy, cost, ease of integration with the existing RIEE, and impact on operations. Selections were based on the ability of a scheme to provide features contributing to one or more of the above benefits: accuracy is improved if the ratio of rack to lift weight is maximized; sensor cost is minimized by using Load Cells; integration is easiest with Load Pins replacing those in the existing RIEE; operations are easier if the Interface Plate (500 lbs.) is included in the lift weight. Separate sensor schemes maximizing each of these desirable features are compared.

Accuracy specifications could only be satisfied for rack weights approaching the upper limit (1750 lbs.) of the load range using "off-the-shelf" sensor equipment. Locating the C.G. within the specified 0.4" was within the capability of "off-the-shelf" sensors.

TABLE OF CONTENTS

| Section | Title | Page |
|------------|---------------------------------|------|
| I | INTRODUCTION | 1-1 |
| 1.1 | Objective | 1-1 |
| 1.2 | Motivation | |
| 1.3 | Scope | |
| 1.4 | Module | |
| 1.5 | Rack | 1-4 |
| 1.6 | Rack Insertion | |
| 1.7 | RIEE | |
| II | SENSOR SCHEMES | 2-1 |
| 2.1 | Alternatives | 2-1 |
| 2.2 | Accuracy | 2-3 |
| 2.3 | Models | 2-4 |
| III | RESULTS | 3-1 |
| 3.1 | Samples | 3-1 |
| 3.2 | Ranges | |
| 3.3 | Accuracies | 3-2 |
| 3.4 | Allowables | 3-3 |
| IV | CONCLUSIONS | 4-1 |
| 4.1 | Summary of Results | 4-1 |
| 4.2 | Conclusions | |
| 4.3 | Recommendations | |
| APPENDIX A | PLATE MOUNTED SENSORS | A-1 |
| APPENDIX B | ARM MOUNTED SENSORS | B-1 |

LIST OF ILLUSTRATIONS

| Figure | Title | Page |
|--------|--|------|
| 1.1 | RACK COORDINATE SYSTEM | |
| 1.2 | END EFFECTOR / MODULE CLEARANCES | |
| 1.3 | C.M. ENVELOPE FOR INTEGRATED RACK with 1543 lbm PAYLOAD | |
| 1.4 | RACK ATTACH POINTS | |
| 2.1 | SENSOR PLACEMENT SCHEMES | |
| 2.2 | RACK & BAR SUSPENSION | |
| 2.3 | ORTHO - STRUT PAIR INTERSECTION | |
| 2.4 | RACK & PLATE SUSPENSION | |
| 2.5 | RACK-PLATE & ARMS SUSPENSION | |

INTRODUCTION

1.1 OBJECTIVE

Design a method to measure weight and center of gravity (C.G.) location for Space Station Resupply Module Racks by adding sensors to the existing Rack Insertion End Effector (RIEE).

1.2 MOTIVATION

Current plans for weight and C.G. measurement require placement of the 1 x 1 x 2 m, half moon shaped racks (weighing as much as 1750 lbs.), Figure 1.1, in a special stand instrumented with load cells. Racks will have to be located on the stand in two positions if two sets of readings are required. Then the racks are to be transferred to the RIEE for installation into the space station resupply module. Measuring weight and C.G. while the rack is attached to the RIEE will eliminate the need for a separate measurement stand. Time will be reduced by one rack reposition and two rack transfer operations.

1.3 SCOPE

Non-experimental assessment of competing sensor placement schemes to determine accuracy, cost, installation and operational characteristics of selected alternatives.

Range of variables:

Specified by NASA:

Accuracy:

| | | | | | |
|-----------------|--------|------|---------|----|---------------|
| Measured weight | within | +/-- | 0.2 % | of | actual weight |
| " C.G. | " | " | 0.4 in. | of | " C.G. |

Constraints:

Rack weight: $250 < W_r < 1750$ lbs.

C.G. envelope: 6.3 x 4.6 x 11.4 ins.

Specified by vendors:

Sensor ranges: 500, 1000, 2000 lbs. (off-the-shelf)

" accuracies: 0.05 % of full scale (" " "maximum)

1.4 MODULE

Space station resupply modules are pressurized cylindrical containments of approximately 4m diameter x 4m length. They contain 16 quarter cylinder, moon shaped segments called racks, Figure 1.2 . Racks are 1m in axial thickness so that 4 sets of 4 segments fill the module. Access to the module is thru a 2.4m diameter hatch in the bulkhead at the end.

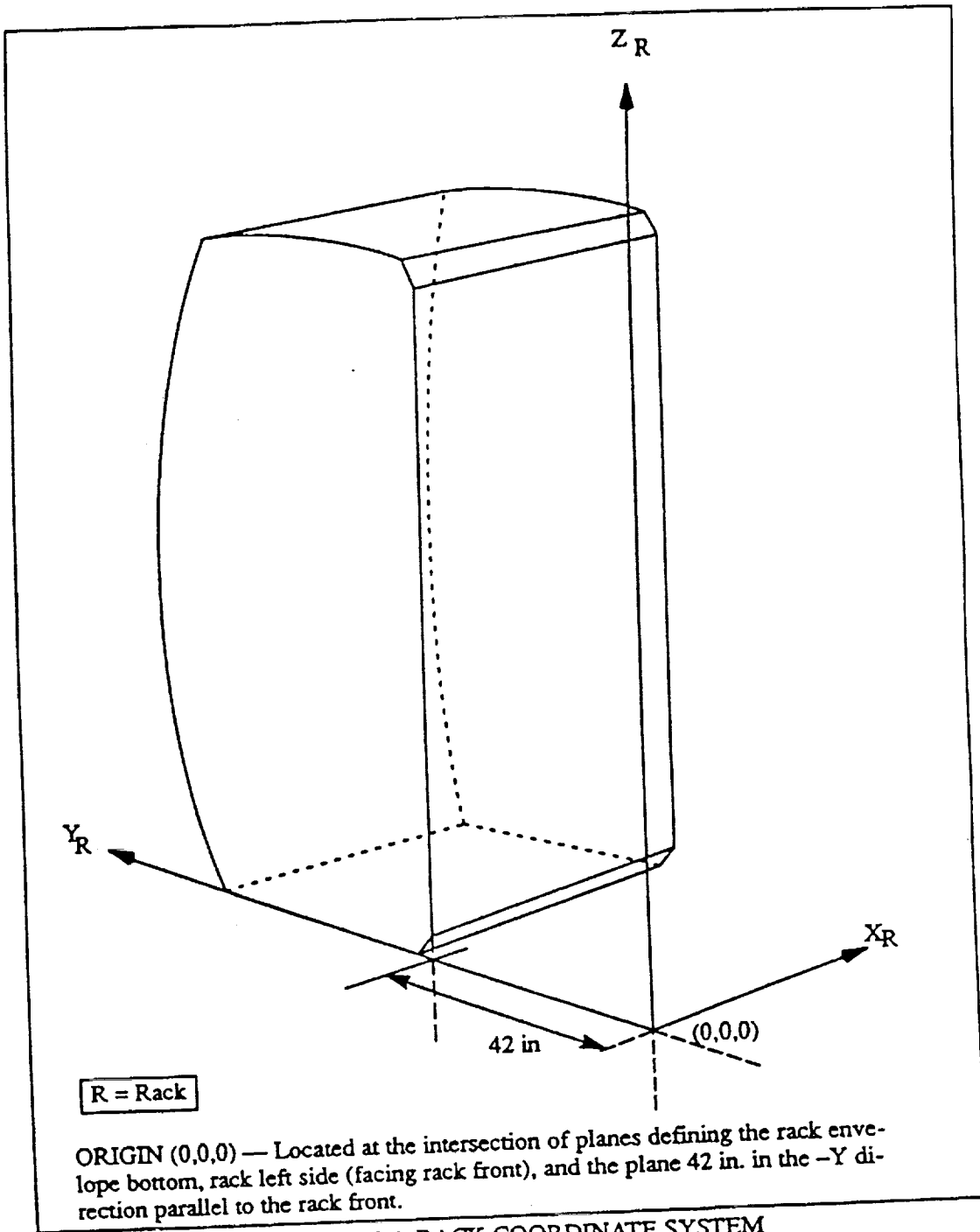


FIGURE 1.1 RACK COORDINATE SYSTEM

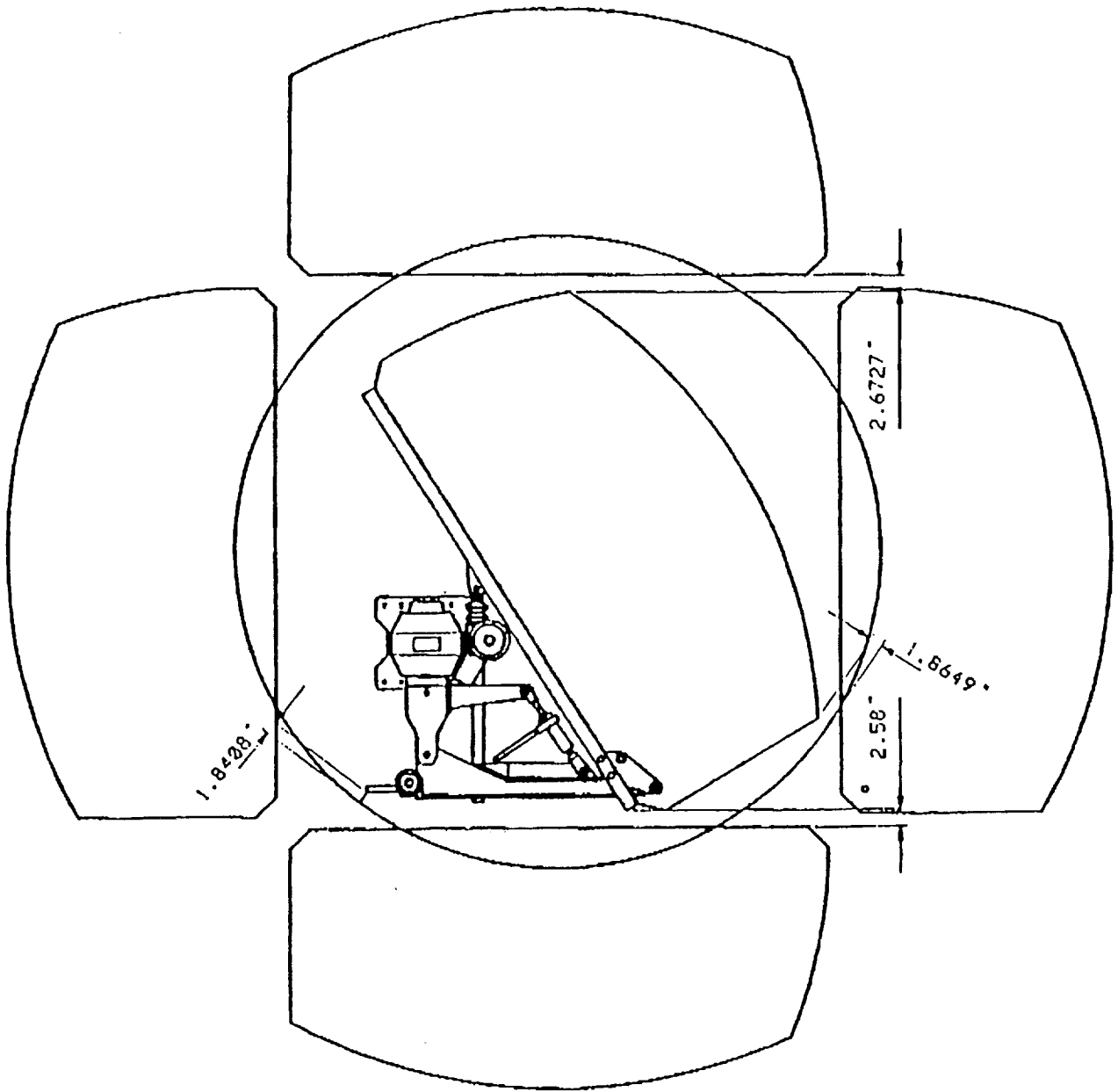


FIGURE 1.2 END EFFECTOR / MODULE CLEARANCES

1.5 RACK

"U.S. Standard Equipment Rack (is described in the) Interface Development Document",[1].

Figure 1.1 shows the coordinate system used for the rack. X_r coordinate measures from the left side of the rack in the direction of the module cylindrical axis. Y_r coordinate measures parallel to a radius, perpendicular to a plane thru the module center line. Z_r measures from the rack base orthogonal to X_r and Y_r .

Figure 1.2 shows the rack attached to the Rack Insertion End Effector (RIEE) in the inclined position necessary for insertion thru the bulkhead access hatch.

Figure 1.3 shows the specified C.M. (Center of Mass is the same as the Center of Gravity, C.G.) envelope for the larger (1543 lbm) of 2 rack specifications. The envelop for the smaller (882 lbm) is slightly more generous.

Figure 1.4 shows the location of Rack Attach Points. Only points G,H,E,F, at the corners of the frontal plane can be used by the RIEE to manipulate the rack.

1.6 RACK INSERTION

Semi-robotic installation of racks into the module is accomplished with a large, 3 d.o.f. (degree of freedom), robotic positioning device supporting a 6 d.o.f., manually operated end-effector weighing 2 tons.

ORU Handling Device is the designation of the robot [2]. Its main feature is a large beam, telescoping in the X_r direction, on which the end-effector is mounted. Smaller Y_r & Z_r translations are permitted.

RIEE is the designation of the manual end-effector [3]. The rack is mounted on the RIEE interface plate by 4 bolts that pass thru holes at the corners of the 1 x 2m plate to screw into threaded holes in the rack at attach points G,H,E,F on the rack front panel. Rack and Plate thus assembled in a vertical position are then tilted by the RIEE to an angle of 35 deg (as on the left in Figure 1.5) so that both may pass thru the module access hatch as shown in Figure 1.2 . On the inside, the rack is returned to vertical as it is placed into its functional location.

1.7 RIEE

Rack and interface plate combination are supported at 3 points. A retractable jack strut between end-effector frame and plate cross-member controls tilt angle. Two variable length arm beams lift pivot points at the base of the plate. These are in turn lifted by 2 turnbuckle tensile struts. Varying degrees of displacement are provided in surge and heave adjustments. Pitch of 35 deg with much smaller amounts of roll and yaw rotations are also accommodated.

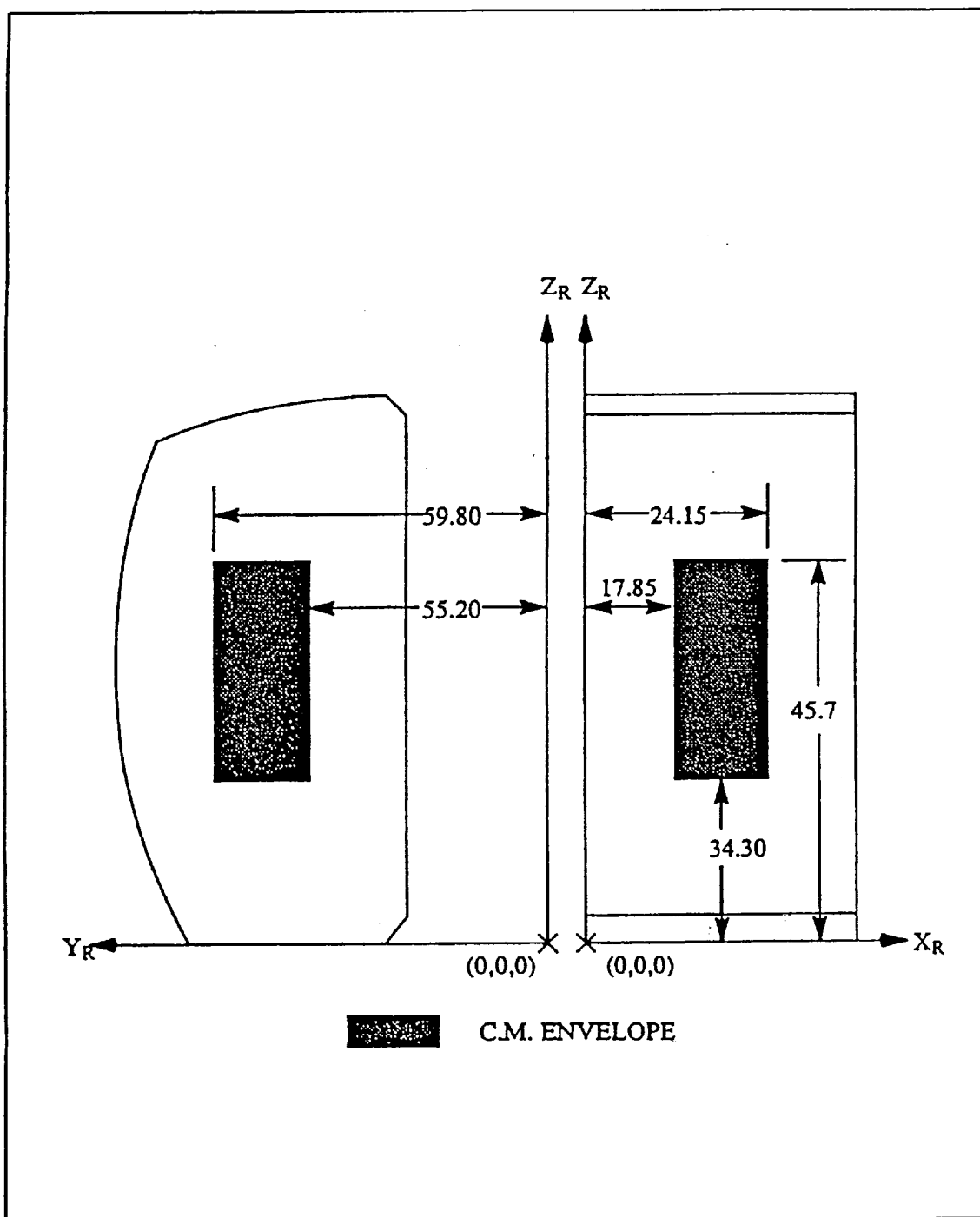


FIGURE 1.3 C.M. ENVELOPE FOR INTEGRATED RACK
WITH 1543 LBM PAYLOAD

| POINT | X_R | Y_R | Z_R |
|-------|--------|--------|--------|
| A | 1.350 | 69.866 | 1.678 |
| B | 40.650 | 69.866 | 1.678 |
| C | 1.260 | 46.020 | 79.315 |
| D | 40.740 | 46.020 | 79.315 |
| E | 1.300 | 42.000 | 2.750 |
| F | 40.700 | 42.000 | 2.750 |
| G | 1.300 | 42.000 | 74.840 |
| H | 40.700 | 42.000 | 74.840 |
| I | 0.500 | 45.500 | 3.800 |
| J | 41.500 | 45.500 | 3.800 |

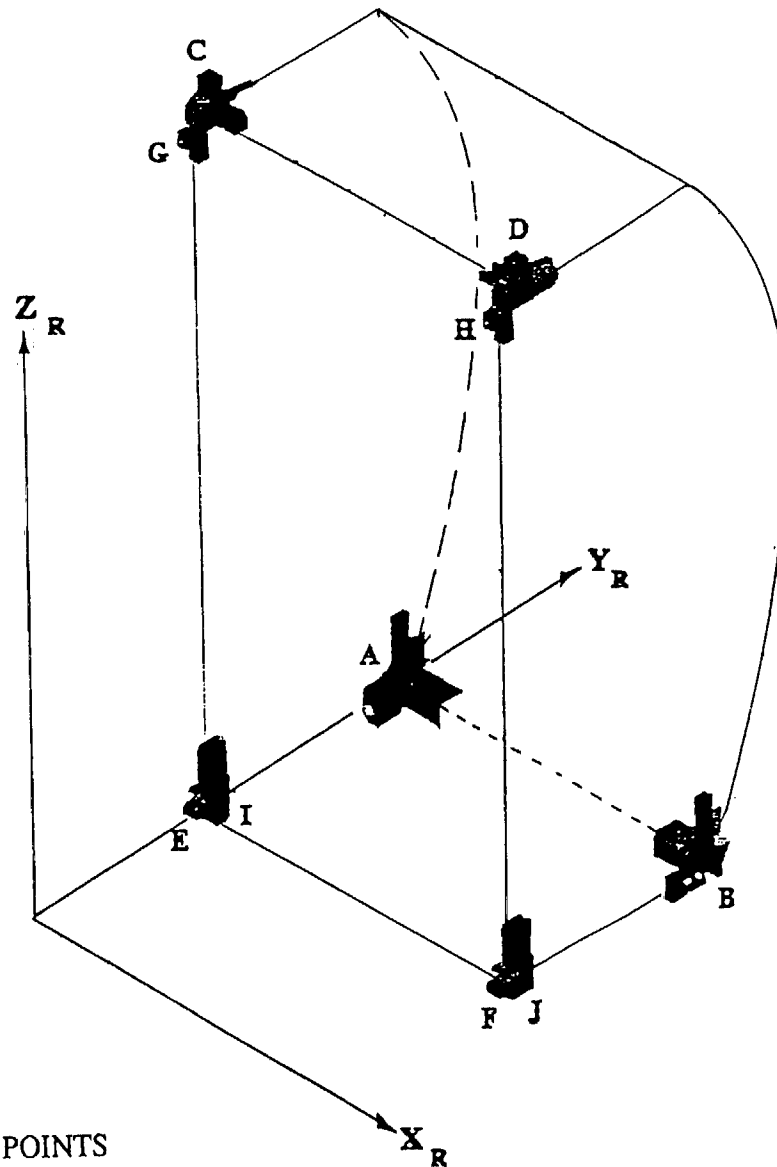


FIGURE 1.4 RACK ATTACH POINTS

II

SENSOR SCHEMES

2.1 ALTERNATIVES

Sensor placement schemes, suggested by interested personnel from NASA/KSC Special Projects Branch / Robotics Laboratory, were organized into 4 categories, Figure 2.1, with some variations on each theme:

2.1.1 ONE BIG F / T. A single, heavy lift, Force / Torque sensor placed between robot and end-effector offers simplicity of installation requiring no modifications to either. Servicing the sensor is facilitated by its location, remote from higher activity areas close to the rack.

Off-the-shelf F/T sensors of the specification required ($F = 4,000$ lbs / $T = 96,000$ lb-ins) are unavailable. Custom construction of such a sensor has been estimated at \$150,000 with a 36" diameter and measurement error on the order of ± 100 lbs.

Another approach calls for building the F/T device from 6 load cells statically arranged in a Stewart Platform configuration. Load cells are relatively inexpensive. Their would be flexibility to trade-off bending against torque capacity using strut angle parameters to achieve a design tailored to this application. I am told this scheme has been tried unsuccessfully before but I have no information on the details of the trial.

2.1.2 TWO PIVOT F / T. Placing sensors at the interface plate pivot points puts them within the commercially available range ($F = 2000$ lbs / $T = 2000$ lb-ins) with several vendors from which to choose. Costs range from \$15 to 30,000 for the pair depending on the extent of customization. Accuracies on the order of 1.0 lb. or less are possible. Choice of 2 computational procedures depends on whether the sensors are fixed to the interface plate, or arm support beam part of the pivot hinges. Some measurement redundancy can be added by installing a load pin at the upper end of the jack strut.

2.1.3 THREE LOAD PINS. Replacing ball-clevis pins in the RIEE with load pins offers the potential of minimum impact on the existing hardware. Cost on the order of \$4,000 renders this the least expensive of all alternatives. Redundant computation is possible but no redundant measurements are available without abandoning the simplicity of just replacing the pins.

2.1.4 FOUR LOAD CELLS mounted in orthogonal pairs at the lower outside corners of the interface plate such that they support only the rack and a load bar, read the lowest lift forces (as seen by sensors), therefore offer the highest potential accuracy. Cost of approximately \$5,000 is expected. Computations for this method (and 2.1.2 interface mounted F/T) do not depend on knowing the plate tilt angles precisely as do other computational methods.

1 BIG F/T sensor
between robot
& end-effector

2 F/T sensors
at interface
plate pivots

SPACE STATION
PROCESSING FACILITY
RACK INSTL/REMOVAL
END EFFECTOR

WEIGHT
&
C.G.
SENSOR SCHEMES

3 Load Pins
replacing
existing pins

4 Load Cells in
2 pairs on
interface plate

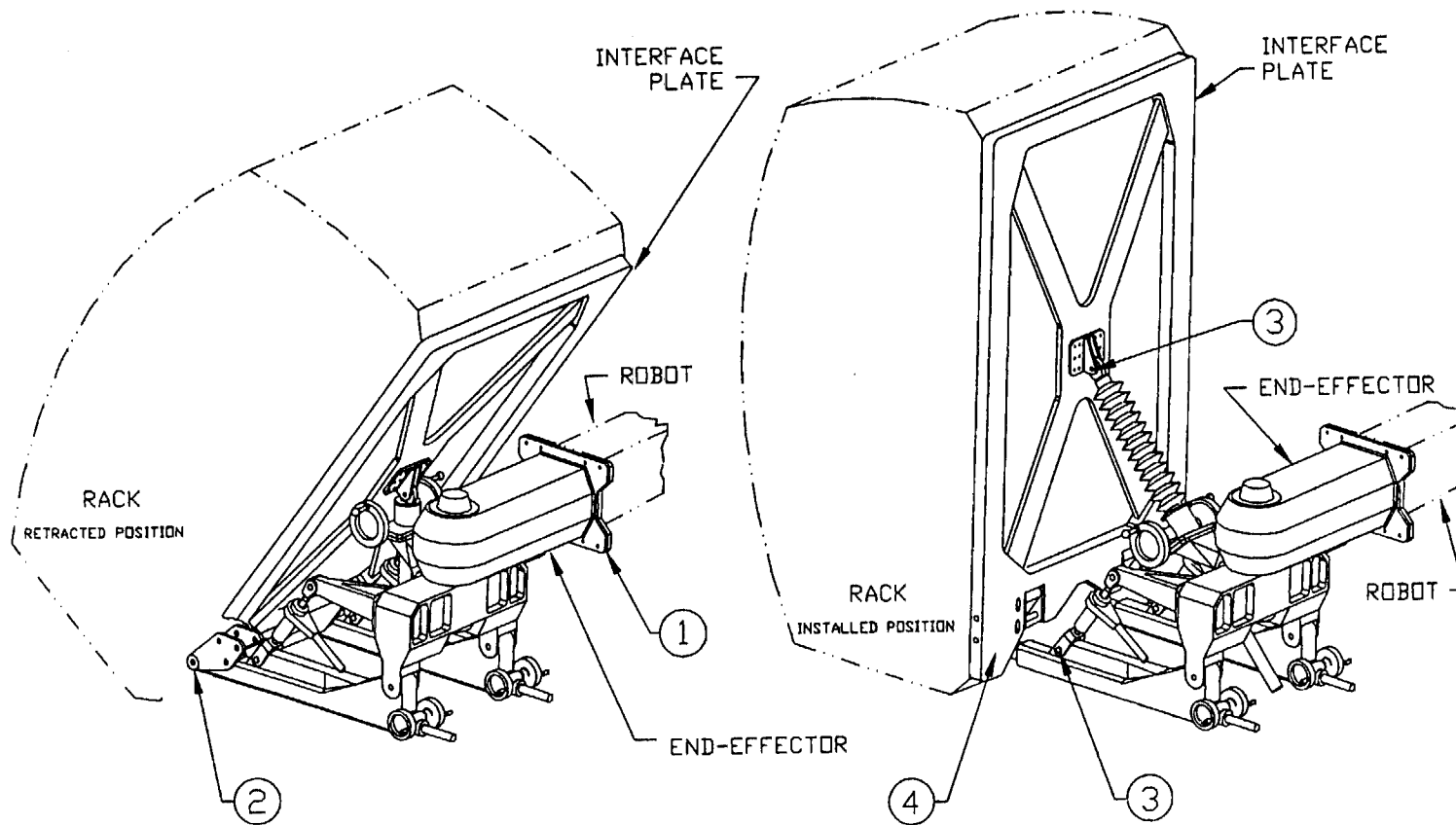


FIGURE 2.1 SENSOR PLACEMENT SCHEMES

2.2 ACCURACY

Sensor scheme error is dependant on component errors in: force measurement, dimensional parameters (c.g. of end-effector parts and load point locations) and friction effects. This non-experimental study attempts to access only the overall effect on accuracy that might be expected as a result of errors in force measurement. Dimensions are still in a state of flux. Approximations have been made, where required, based on information made available. No attempt has been made to measure or quantify errors that may be introduced by dimensional uncertainty or friction in suspension linkages.

2.2.1 RANGE DEPENDANCE. Scheme accuracy is dependant on component sensor error. Sensor load range must be specified before error (almost universally a % of range) can be known. Range is determined by the maximum load a sensor will experience over the total measurement process. An inverse computation (i.e. given rack weight and C.G. location, find forces in the end-effector where sensors are located) is used to establish range information. This is done by assuming the maximum allowable rack weight and C.G. off-set (from geometric symmetry plane of both rack and end-effector). Sensor placements that result in statically indeterminant inverse solutions make range determination a function of structural rigidity. This would be true, for example, with sensors placed between rack and plate at all 4 Rack Attach Points in Figure 1.4 . Simplicity suggests these be excluded from consideration.

2.2.2 SENSOR SELECTION. Nominal range specifications are usually in increments of 100, 500, 1000, 5000 etc. for off-the-shelf equipment. Maximum expected sensor load is thus rounded up to the nearest available range. This and the physical sensor dimensions that will fit in the space available are absolute requirements. Beyond these, trade-offs between cost, accuracy, availability, service, ease of installation and operation are among considerations that are less clear cut.

2.2.3 SENSOR ACCURACY. Error components are normally broken down into various categories: non-linearity, hysteresis, non-repeatability, temperature effects on output and zero. These are usually expressed as a percent of the specified full scale sensor range. An overall error parameter is obtained by combining the various categories as the square root of the sum of squared component values. This emphasizes larger error sources and minimizes the impact of minor ones. It is less conservative than simple summation of component errors.

2.2.4 SCHEME ACCURACY. Forces at sensor locations are found using the inverse solutions discussed in 2.2.1 above. The overall error parameter multiplied by the sensor range at each sensor location is added to the force there computed from the inverse solution. Thus modified to reflect possible error, these forces are inputs to the forward solutions resulting in an estimate(s) of weight and C.G. location. Comparison with the original values, assumed as inputs to the inverse solution, yields an estimate of errors the chosen sensor scheme might produce. These can be compared with specified allowable error. Maximum error can be explored by examining the extremes of allowable weight at the vertices of the C.G. envelope.

2.3 MODELS

2.3.1 IMPLEMENTATION. All model computations were made with MathCAD version 2.5. Final models to be used with the hardware should include "if - then" logic for testing +/- conditions. This would allow a better assessment of "worst case" accuracy where force errors combine with true values so they amplify rather than cancel thus reflecting maximum error that may be expected. Further investigation would be expedited with "do-loop" capability.

As matters stand, force error magnitude is merely added to the actual force regardless of its sign. To obtain maximum possible error estimates, manual insertion of error signs is required after signs of actual forces have been computed. Exploration of all possibilities would result in a sizable matrix of solutions. Time permits only sample solution development with tools currently being used. Sample computations are appended and referenced where appropriate.

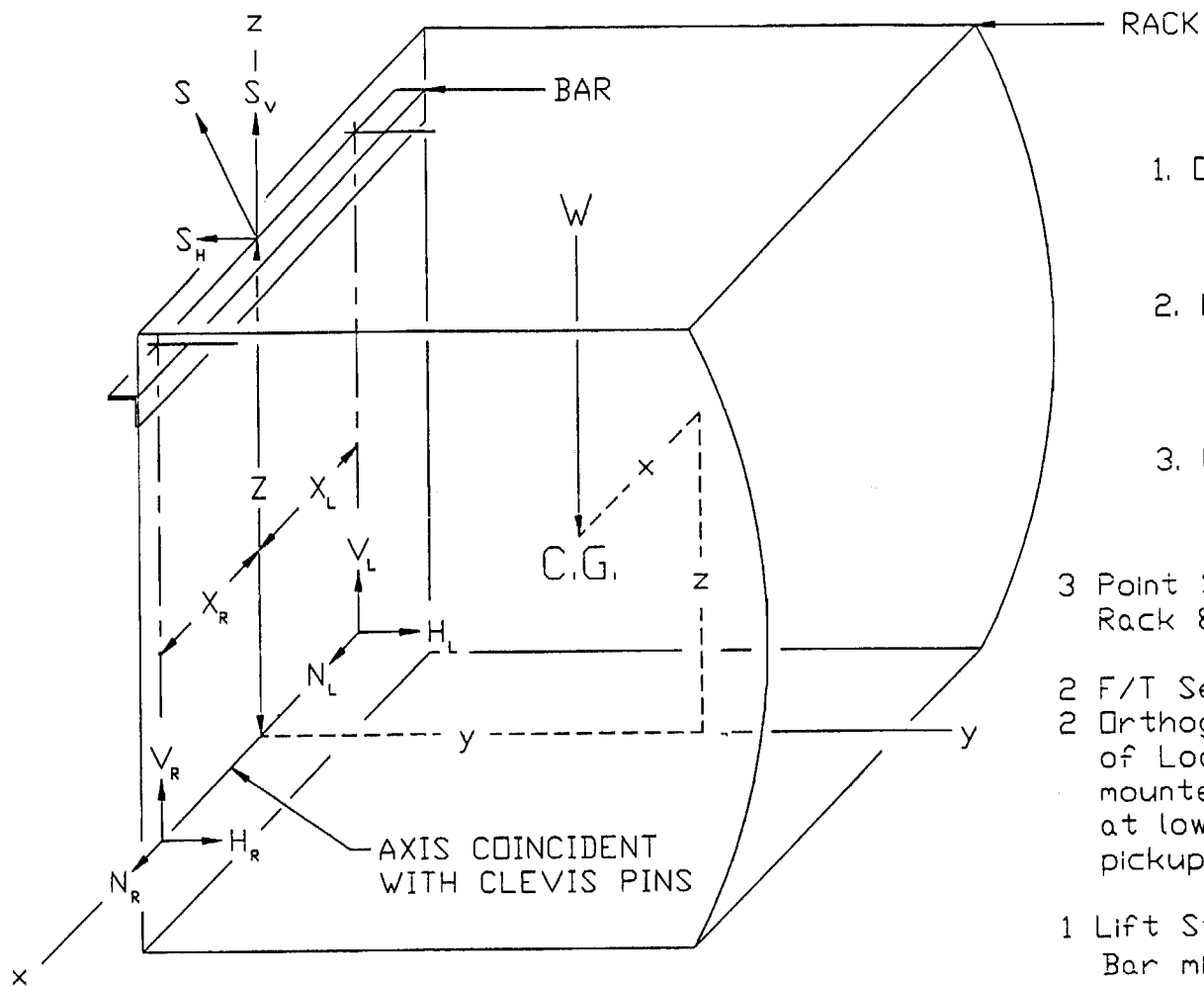
2.3.2 SAMPLES. Preliminary investigation indicated the most difficult specification to satisfy would be measuring weight to within .2% of the actual value as the rack approaches an empty weight ($W_r=250$ lbs). As the ratio of pay-load / lift-load approaches zero the errors become unbounded. For this reason schemes that minimize tare weight are considered first:

2.3.2.1 Rack Alone. Suspension of the rack alone was not possible within given constraints. Suspension from the 4 attach points shown in Figure 1.4 and discussed in section 1.5 above would result in a statically indeterminate problem rendering an inverse model difficult to solve. Using only 3 attach points would be determinant. This was disallowed because such an asymmetric lift could distort (or deform) the rack frame.

2.3.2.2 Rack & Bar. Approximation of rack alone suspension uses a lift bar spanning the upper 2 attach points, Figure 2.2. A bar-mounted, load bearing strut is placed perpendicular to the longitudinal axis of the bar at its middle. This allows a symmetric, 3 point, determinant suspension. Strut angle can be adjusted to balance loads on sensors as the interface plate moves from the vertical to an inclined position. Reduction of the required load range to improve accuracy is the result. A load cell in this strut would supply a redundant reading as a check.

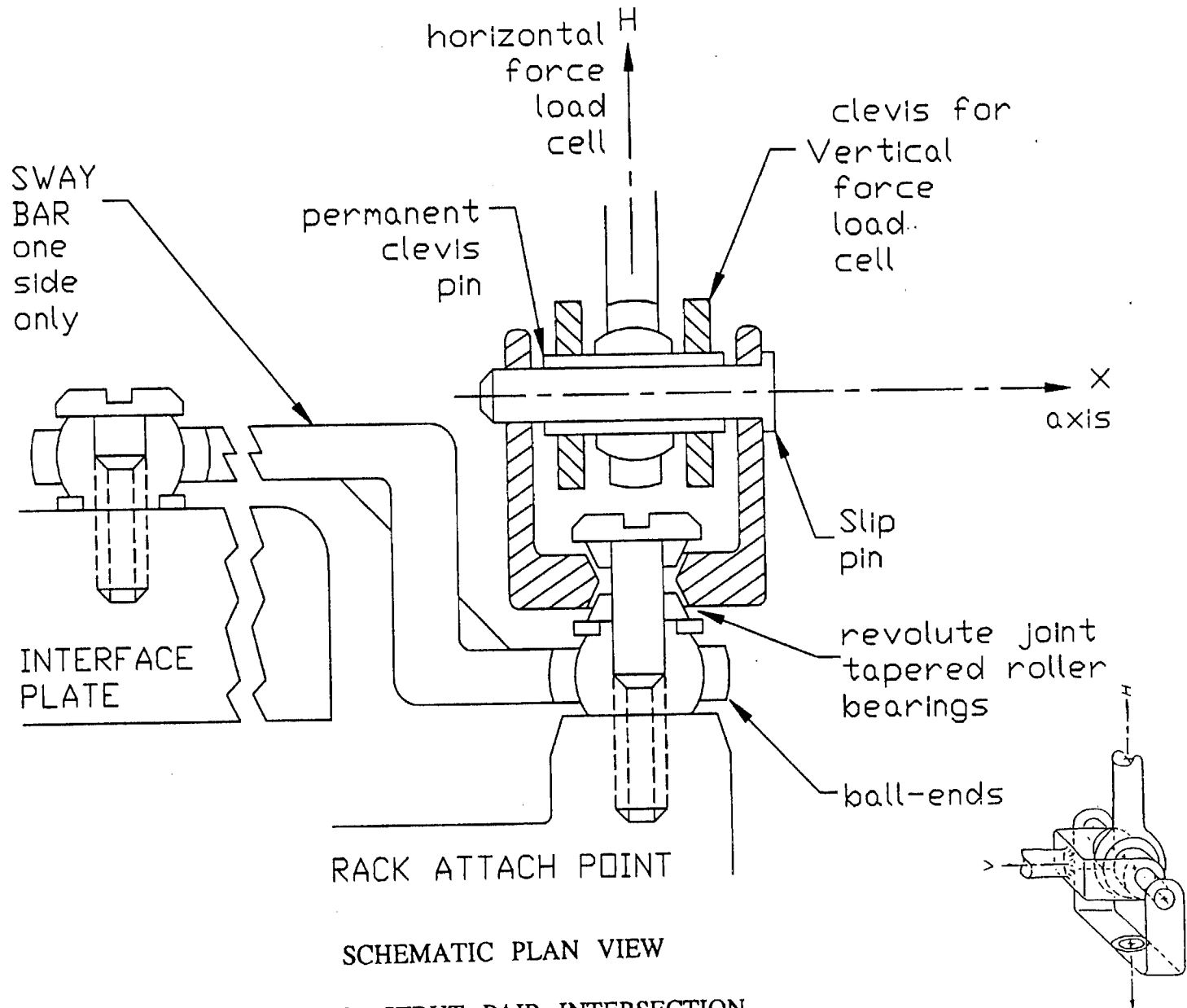
Orthogonal pairs of load cell struts between rack and interface plate at the lower attach points completes the suspension and measurement scheme. Suspension of the rack without bolting it to the interface plate presents some installation and operational complications. An adequate, determinant suspension would permanently join the pair of ball/clevis ended ortho-struts to each other at a single ball with a hollow pin, Figure 2.3 . An additional clevis yoke would be bolted to the rack attach point with a revolute joint between. At the time of mating rack to plate, this yoke would be attached to the permanently assembled ortho-struts with a "slip-pin" thru the permanent hollow pin. This arrangement allows both concentric clevis pins to share the same axis. A "sway bar" along the plate bottom constrains the ortho-strut pairs so their axes remain in a vertical plane, Figure 2.3 . An alternative to load cells substitutes a single F/T sensor for each load cell pair. Only one ball/clevis at each location is required. See Appendix A.

3 Point Suspension Scheme RACK & BAR Plate Mounted Sensors



- NOTE
1. ONLY fixed dimensions required
 2. NO Angle of inclination measurements required
 3. LOW lift weight
- 3 Point Suspension of Rack & Support Bar
 - 2 F/T Sensors or 2 Orthogonal Pairs of Load Cells mounted on Plate at lower Rack pickup points
 - 1 Lift Strut at Bar mid-point

FIGURE 2.2 RACK & BAR SUSPENSION



SCHMATIC PLAN VIEW
FIGURE 2.3 ORTHO - STRUT PAIR INTERSECTION

2.3.2.3 Rack & Plate. Bolting rack to plate as intended by the RIEE designers simplifies the attachment operation. Plate weight of 500 lbs increases the lift and therefore sensor range required. Modification of the plate, though not required, would be beneficial if the tare weight could be significantly reduced. The rack-plate unit may be treated as a 3 point determinant suspension with the jack-strut supporting in the middle of the plate and 2 plate-pivot hinges providing reactions at the bottom of the plate, Figure 2.4. One F/T sensor at each pivot hinge is sufficient to extract all necessary information. A load-pin at the upper end of the jack would give a redundant check.

Plate mounted sensors may be attached to the plate side of the pivot hinge. Model computations would be similar to those in Appendix A for the Rack & Bar case but with different geometric parameters and mass combinations. Since the sensors tilt with the rack-plate so does the reference frame. The sensors see a weight vector that changes its angle of incidence equal to the tilt. Plate angles need not be known (except for the redundant check) but should be separated as far as possible.

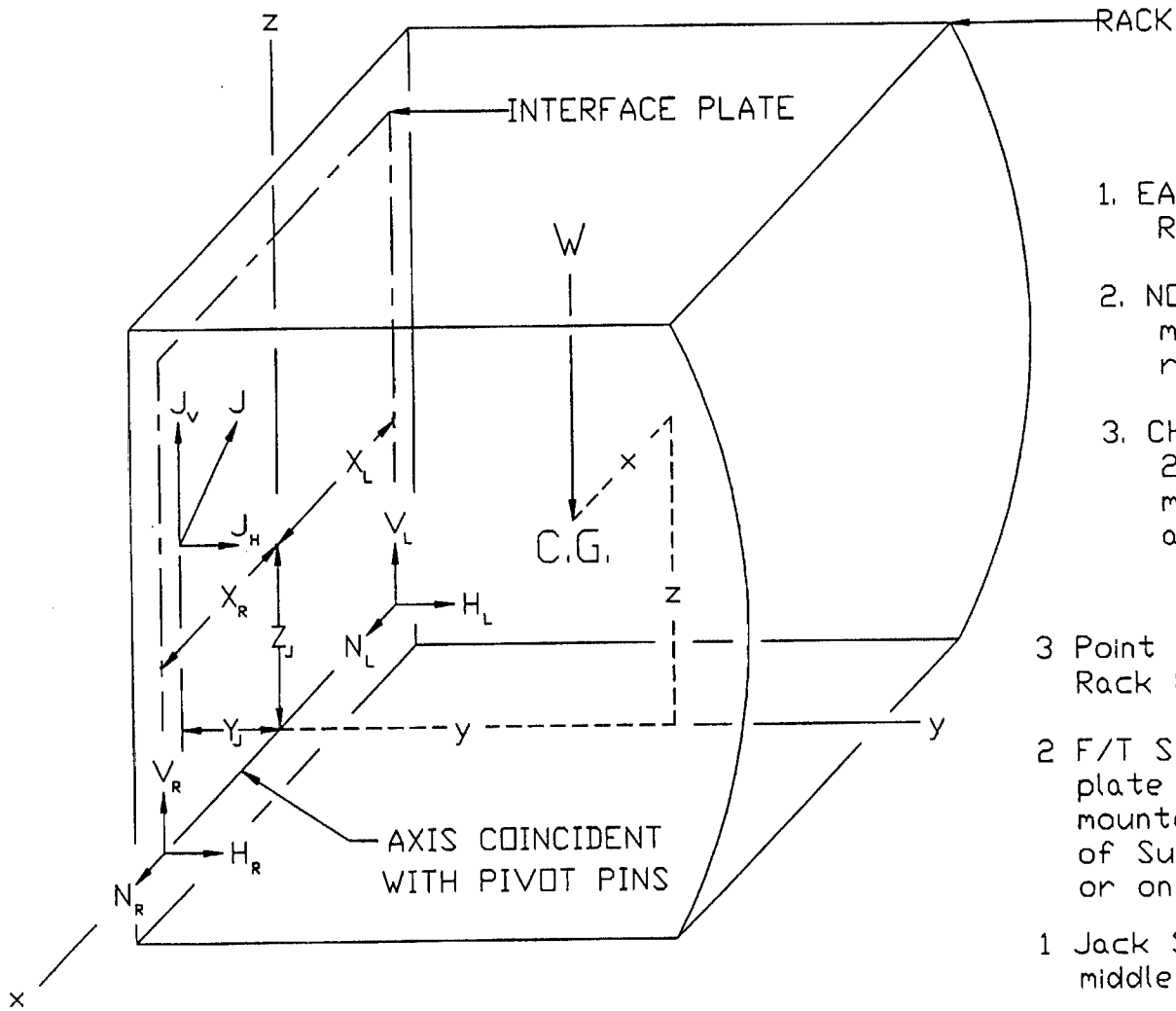
Arm mounted sensors may be attached to the arm side of the pivot hinge. Model computations are given in Appendix B. Sensors are fixed as is the reference frame. When the plate tilts, computational procedure is the same but a coordinate transformation is required to relate back to the vertical position of the plate. The method depends on interface-plate and jack-strut angles, one set of which must be for the vertical position. This introduces an additional source of operational error. Information on expected angular measurement error is not currently available. Accuracy assessments made here do not reflect this possibility.

2.3.2.4 Rack-Plate & Arms. Replacement of existing ball-clevis pins with load-pins would require the least modification of existing hardware. Load pins are unidirectional. If the direction of applied load differs from pin orientation by more than 15 deg, readings are unpredictable. This limits their use to struts (i.e. 2-force members) where the load direction is known to be parallel to a line between the end attach points. Plate pivot and arm-elbow pins do not qualify. A 5-point suspension of 3 rigid members, consisting of the rack-plate and both arms, is determinant. Pins are replaced at the jack-strut upper end and lower ends of the 2 turnbuckle struts. These 3 members are the only 2-force members in the end effector. They are sufficient for all computations. Any attempt at adding redundancy would destroy the simplicity of the installation. More geometric information is required for this computation than the previous ones. It depends, as does the Rack & Plate with arm mounted sensors, on the accuracy of angles, locations of plate & arm centers of mass, and load points, Figure 2.5. It is difficult to obtain both forward and inverse solutions from the Rack-Plate & Arms taken as a single unit. Rather writing equations for the individual members is more fruitful especially since the solutions for the Rack & Plate in Appendix B can be used as part of the solution for this problem together with additional equations representing the arm beams.

2.3.2.5 Higher Tare Weights. All other schemes involving higher lift weights have not been evaluated because of the adverse trend of error measured as a percent of rack weight.

3 Point Suspension Scheme RACK & PLATE

Arm or Plate Mounted Sensors



NOTE

1. EASY 4 bolt Rack mounting
2. NO plate modifications required
3. CHOICE of 2 sensor mount/compute arrangements

- 3 Point Suspension of Rack & Plate
- 2 F/T Sensors at plate pivots mounted on ends of Support Arms or on Plate Hinge
- 1 Jack Strut behind middle of Plate

FIGURE 2.4 RACK & PLATE SUSPENSION

ASSUMPTIONS
during all sensor readings

1. Pin axes horizontal
2. Arm axes horizontal
3. y-z plane is vertical
4. y-z plane is a plane of interface plate symmetry
5. Both symmetry planes of interface plate are vertical
 $l = 0$

Rack Weight & C.G. SENSOR SCHEME
5 Point Suspension

Coordinate Origins
and
Geometric Parameter
Identification

NOTE

5 point scheme depends on
RELATIVE
rather than only
FIXED
dimensions

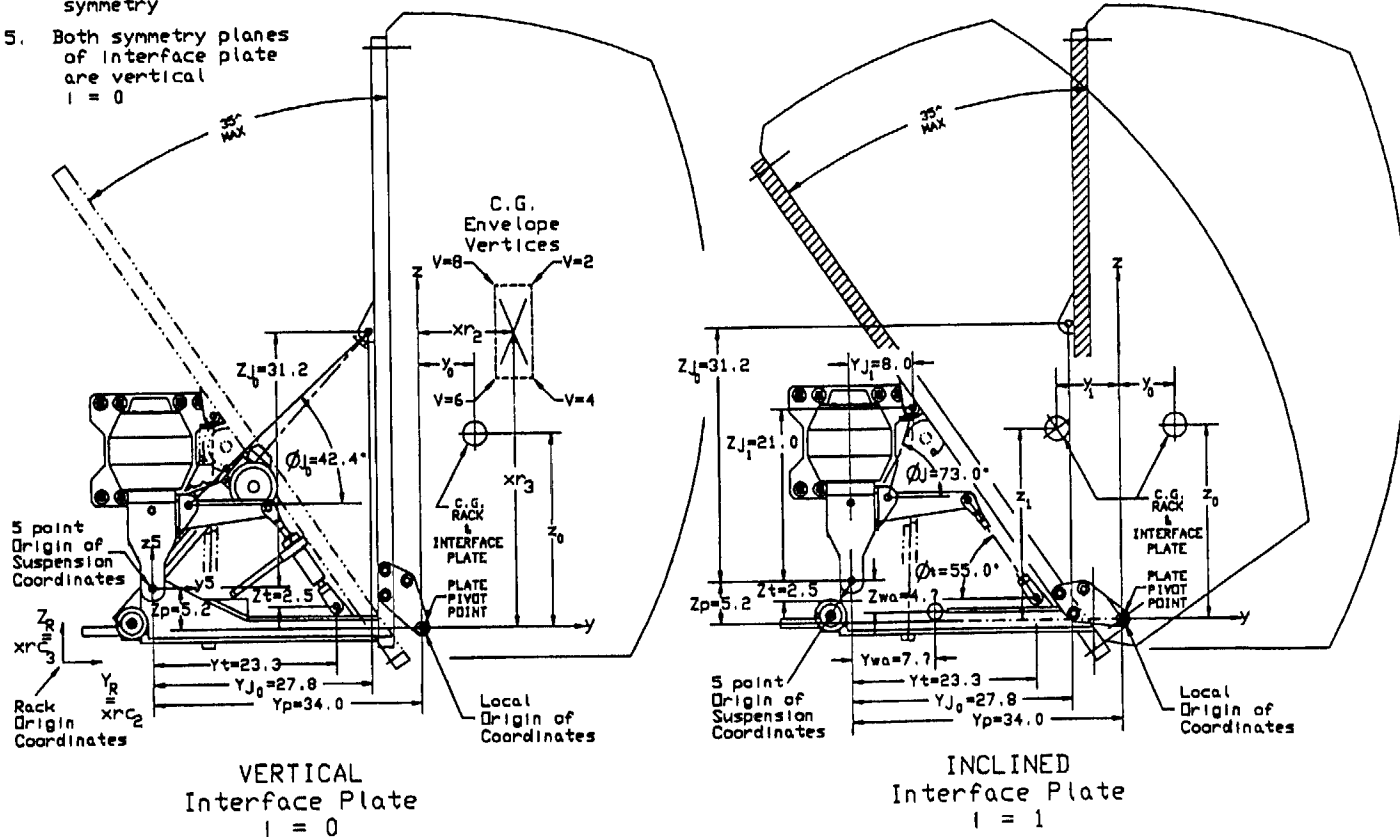


FIGURE 2.5 RACK-PLATE & ARMS SUSPENSION

III
RESULTS

3.1 SAMPLES

Computations exhibited in the appendices were for the largest rack weight with a maximum allowed off-center C.G. at an upper right vertex No. 2. These give a good indication of maximum sensor load. Sensor ranges were determined by rounding up to the next available size. Vendors were queried for suitable sensor equipment recommendations.

3.2 RANGES

3.2.1 RACK & BAR. (with the least tare weight has the lowest ranges)

| | | | |
|---------------------------|-------------|----------------|----------|
| Vertical Load Cell range: | 913 lbs max | rounded up to: | 1000 lbs |
| Horizontal " " " : | 490 " " | " " " | 500 " |

3.2.2 RACK & PLATE.

| | | | |
|---------------------|--------------|----------------|----------|
| Vertical F/T range: | 1592 lbs max | rounded up to: | 2740 lbs |
| Horizontal " " " | 197 " " | " " " | 1140 " |

Note: The F/T data is for a custom sensor. It is a package that does not allow independent choice of vertical and horizontal force ranges. To achieve the indicated performance this 3.1" diameter unit must be oriented with its axis in the direction of maximum load. It may be worth exploring the possibility of a custom F/T sensor with lower ranges that are closer to those needed.

3.2.3 RACK - PLATE & ARMS.

| | | | |
|----------------------------|-------------|----------------|----------|
| Jack Strut Load Pin range: | 994 lbs max | rounded up to: | 1000 lbs |
| Turnbuckle " " " | 3313 " " | " " " | 3500 " |

Note: Ranges for off-the-shelf Load Pins were 1500, 3000, 6000 lbs which are so far from the required ranges as to prejudice any comparison with the other alternatives. Values shown were substituted assuming that custom load pins would be possible and worth the effort if this case is selected for further development.

3.3 ACCURACIES

3.3.1 MAXIMUM RACK WEIGHT. The best accuracies are expected using the load for which the range was selected, $W_r=1750$ lbs. The sample calculations in the appendices compute these results for Vertex 2 of the C.G. envelope ($x_r=24.15$, $y_r=59.80$, $z_r=45.7$).

Note that two estimates, one for each plate angle, are produced for most quantities. However when the sensors are plate mounted, equations from both plate positions are needed to obtain a single assessment of the y and z-coordinates.

| | | | | |
|---------|-------------|-----------------------|-------------------------------------|----------------|
| 3.3.1.1 | Rack & Bar. | erWr = .074 %, .064 % | compared with | .2 % allowable |
| | | erx = -.002 in. both | " " | .4 in. " |
| | | ery = .006 " | " " | " " |
| | | erz = .009 " | " " | " " |
| | | erv = .011 " | (vector sum of coordinate errors) | |

Weight error is about a third of that allowed.

C.G. error is more than an order of magnitude less than the requirement.

| | | | | |
|---------|---------------|---------------------------|-------------------------------------|----------------|
| 3.3.1.2 | Rack & Plate. | erWr = .059 %, -.164 % | compared with | .2 % allowable |
| | | erx = -.001 in., .003 in. | " " | .4 in. " |
| | | ery = .016 " .035 " | " " | " " |
| | | erz = .038 " .022 " | " " | " " |
| | | erv = .041 " .041 " | (vector sum of coordinate errors) | |

Weight error is about a third of that allowed.

C.G. error is about an order of magnitude less than the requirement.

| | | | | |
|---------|-----------------------|----------------------------|-------------------------------------|----------------|
| 3.3.1.3 | Rack-Plate & Arms. | erWr = 1.839 %, 1.928 % | compared with | .2 % allowable |
| | | erx = -.035 in., -.036 in. | " " | .4 in. " |
| | | ery = -.242 " .118 " | " " | " " |
| | | erz = -.551 " -.590 " | " " | " " |
| | | erv = .603 " .603 " | (vector sum of coordinate errors) | |

Weight error violates the allowable by nearly an order of magnitude.

C.G. error violates the allowable by about 50 %.

3.3.2 DATA TREND. For these three quite different sensor placement schemes, desirable performance correlates inversely with sensor range and directly with the ratio of pay-load / lift-load. These are, of course, both manifestations of the same phenomenon.

Correlation with the pay/lift ratio is very evident as it approaches zero.

3.3.3 MINIMUM RACK WEIGHT. The worst accuracies can be expected with minimum rack weight, $W_r=250$ lbs. Results given below are for Vertex 2 of the C.G. envelope.

Note the envelope for smaller rack weights of mass less than 882 lbm, is larger than that for maximum rack weight. Vertex 2 moves out to ($x_r=26.50$, $y_r=61.50$, $z_r=50.00$).

3.3.3.1 Rack & Bar. $erW_r = .515 \%$, $.448 \%$ compared with $.2 \%$ allowable
 $er_x = -.020$ in., $-.017$ in. " " $.4$ in. "
 $er_y = .039$ " " " "
 $er_z = .024$ " " " "
 $er_v = .050$ " (vector sum of coordinate errors)

Weight error is more than double the allowable.
 C.G. error is less than allowed by nearly an order of magnitude.

3.3.3.2 Rack & Plate. $erW_r = .411 \%$, -1.166% compared with $.2 \%$ allowable
 $er_x = -.003$ in., $.007$ in. " " $.4$ in. "
 $er_y = .053$ " $.165$ " " " "
 $er_z = -.212$ " $-.143$ " " " "
 $er_v = .219$ " $.218$ " (vector sum of coordinate errors)

Weight error is more than double the allowable.
 C.G. error is about half of that allowed.

3.3.3.3 Rack-Plate & Arms. $erW_r = 12.87 \%$, 13.50% compared with $.2 \%$ allowable
 $er_x = -.075$ in., $-.079$ in. " " $.4$ in. "
 $er_y = -.385$ " $.547$ " " " "
 $er_z = -1.503$ " -1.452 " " " "
 $er_v = 1.553$ " 1.554 " (vector sum of coordinate errors)

Weight error violates the allowable by more than an order of magnitude.
 C.G. error violates the allowable by nearly a factor of 4.

3.4 ALLOWABLES

Data presented indicates that it is much easier to satisfy the absolute limit for C.G. error of $.4$ in than the variable $.2 \%$ error for the weight. The problem is measurement range. Percent error is a difficult standard to apply to measurement when the range of interest approaches zero. If zero is included it is impossible. The cost is not accompanied by a commensurate benefit. Empty racks are less likely to affect the overall resupply module's weight and C.G. yet the cost of their measurement is likely to be high if error is expressed as a fixed percent of the true value.

IV CONCLUSIONS

4.1 SUMMARY OF RESULTS

- o Three models representing different sensor placement schemes, each with its own computational method, were developed.
- o Inverse solutions, assuming known weight and C.G. location extremes, were used to determine maximum expected sensor load so that sensor load ranges could be selected.
- o Forward solutions predict overall expected sensor error from each scheme based solely on component errors of sensors employed. Other error sources such as friction, dimensional and angular measurement error were not investigated.

4.2 CONCLUSIONS

- o Sensor load range is the major determinant of component sensor error. Lift weight determines load range therefore low lift weight is desirable.
- o Error limits are easily satisfied for the highest rack weights but are far more difficult to satisfy for an empty rack.
- o Error as a percent of weight increases rapidly as the weight approaches zero. It becomes unbounded if the load range includes zero.
- o Cost of measuring near empty racks to the current specification is not accompanied by a commensurate benefit.

4.3 RECOMMENDATIONS

- o Retain the simple four bolt mating of rack to interface plate as intended by the designers of the rack insertion end effector.
- o Isolate the rack-plate with plate mounted force/torque sensors at the plate pivots.
- o Lighten the interface plate.
- o Negotiate fixed error limits based on maximum or expected rack weights rather than the current variable limits based on percent of weight measured.

APPENDIX A
 PLATE MOUNTED SENSORS
 3 Point Suspension of Rack and Bar
 with Inclined Central Support Strut

Vertex := 2

INVERSE COMPUTATION

Weights: Rack: $W_r := 1750$ lbs. Support Strut Bar: $w_b := 50$ lbs.
 Total Lift: $W := W_r + w_b$ lbs.
 Angle of Tilt: $i := 0 \dots 1$ $W = 1.8 \cdot 10^3$ lbs.
 Angle of Strut: $\phi := 30 \cdot \text{deg}$ $\theta := 0$ deg := $\frac{\pi}{180}$

Center of Mass Location: Local Rack Coordinates: Support Strut Bar Coordinates:
 $x_{rc} :=$ $x_r := x_{rc} - 21$ $x_b :=$

| |
|-------|
| j |
| 24.15 |
| 59.80 |
| 45.70 |

| |
|---|
| 1 |
| 1 |
| 2 |
| 2 |
| 3 |
| 3 |

| |
|------|
| j |
| 0.0 |
| 0.0 |
| 72.0 |

 Total Lift Coordinates: $x_t := \frac{x_r \cdot W_r + x_b \cdot w_b}{W}$ x_t

| |
|--------|
| j |
| 3.062 |
| 20.222 |
| 43.757 |

Center of Mass Location: $x := x_t_1$ $y := x_t_2$ $z := x_t_3$
 Load Point Distances: $X := 19.7$ $Y := 0.0$ $Z := 72.0$
 Weight Components: $W_{y_i} := W \cdot \sin[\theta_i]$ $W_{z_i} := W \cdot \cos[\theta_i]$

Reaction at Strut: $S_i := \frac{y \cdot W_{z_i} - z \cdot W_{y_i}}{Z \cdot \cos(\phi)}$

| |
|----------------|
| S _i |
| 583.765 |
| -246.323 |

Reactions Right: $V_{r_i} := \frac{W_{z_i}}{2} \left[1 + \frac{x}{X} \right] - \frac{S_i}{2} \sin(\phi)$ $H_{r_i} := \frac{W_{y_i}}{2} \left[1 + \frac{x}{X} \right] + \frac{S_i}{2} \cos(\phi)$

| |
|----------------------------|
| V _{r_i} |
| 893.97 |
| 913.426 |

| |
|----------------------------|
| H _{r_i} |
| 252.778 |
| 489.808 |

Reactions Left: $V_{l_i} := V_{r_i} - \frac{x}{X} \cdot W_{z_i}$ $H_{l_i} := H_{r_i} - \frac{x}{X} \cdot W_{y_i}$

| |
|----------------------------|
| V _{l_i} |
| 614.148 |
| 684.209 |

| |
|----------------------------|
| H _{l_i} |
| 252.778 |
| 329.308 |

Vertex = 2
3
Wr = 1.75 · 10

3 Point Suspension of Rack and Bar
with Inclined Central Support Strut

FORWARD COMPUTATION

Measurement Error Allowance: Load Cell Accuracy: Ac := .05 %
Force Error: Range: Vrng := 1000 Hrng := 500 lbs
 $\delta V := Vrng \cdot \frac{Ac}{100}$ $\delta H := Hrng \cdot \frac{Ac}{100}$

Reaction Readings with Maximum Errors:

$$Vr_i := Vr_i + \delta V \quad Hr_i := Hr_i + \delta H \quad Vl_i := Vl_i + \delta V \quad Hl_i := Hl_i + \delta H$$

Reaction Combinations:

Reaction Differences:

$$Vs_i := Vr_i + Vl_i \quad Hs_i := Hr_i + Hl_i \quad Vd_i := Vr_i - Vl_i \quad Hd_i := Hr_i - Hl_i$$

Reaction at Strut,
Computed:

$$S_i := \frac{Vd_i \cdot Hs_i - Vs_i \cdot Hd_i}{Vd_i \cdot \cos(\phi) + Hd_i \cdot \sin(\phi)}$$

$$S_i = \begin{matrix} 584.343 \\ -246.488 \end{matrix}$$

Weights, Computed:

$$Wy_i := Hs_i - S_i \cdot \cos(\phi) \quad Wz_i := Vs_i + S_i \cdot \sin(\phi)$$

$$Wyz_i := \sqrt{Wy_i^2 + Wz_i^2}$$

$$Wyz = \begin{bmatrix} 1.801 \cdot 10^3 \\ 1.801 \cdot 10^3 \end{bmatrix}$$

Center of Mass,
Computed:

$$xv_i := \frac{X}{Wz_i} \cdot Vd_i \quad xh_1 := \frac{X}{Wy_1} \cdot Hd_1$$

$$xv_i = \begin{matrix} 3.06 \\ 3.061 \end{matrix}$$

$$y01 := y \quad z01 := z$$

$$xh_1 = 3.061$$

1
xh = singular
0

Given

$$y01 \cdot Wz_0 - z01 \cdot Wy_0 = Z \cdot S \cdot \cos(\phi)$$

$$y01 \cdot Wz_1 - z01 \cdot Wy_1 = Z \cdot S \cdot \cos(\phi)$$

$$\begin{bmatrix} y01 \\ z01 \end{bmatrix} := \text{Find}(y01, z01)$$

$$y01 = 20.228$$

$$z01 = 43.766$$

Vertex = 2
 3
 Wr = 1.75 · 10

3 Point Suspension of Rack and Bar
 with Inclined Central Support Strut

page 3

ERROR ESTIMATES

Weight Error:

Center of Mass Error:

$$erWr_i := \frac{Wyz_i - W}{Wr} \cdot 100$$

$erWr_i$

| |
|-------|
| 0.074 |
| 0.064 |

 % compared with allowable
 .2 %

$$erx_i := xv_i - x_i$$

erx_i in.

| |
|--------|
| -0.002 |
| -0.002 |

 compared with allowable
 .4 in.

$$ery := y_{01} - Y$$

$$erz := z_{01} - z$$

$ery = 0.006$
 $erz = 0.009$
 .4 in.

APPENDIX B

ARM MOUNTED SENSORS

Rack & Plate, 3 Point Suspension
with Inclined Central Support Jack

Vertex := 2

INVERSE COMPUTATION

Weights: Rack: $W_r := 1750$ lbs. Plate: $W_p := 500$ lbs.
 Total Lift: $W := W_r + W_p$ Indices: $i := 0..1$ $j := 1..3$
 $W = 2.25 \cdot 10^3$ Conversion: $\text{deg} := \frac{\pi}{180}$

Angles: Plate: $\theta :=$ Jack: $\phi :=$

Angle of Strut:

| | |
|----------|---|
| 0.00 deg | ? |
| 35.0 deg | ? |

| | |
|----------|---|
| 44.2 deg | ? |
| 78.5 deg | ? |

Center of Mass Location:

| | | | | | | | | |
|--|------------------------------------|--|-------|----------------------------|--|-----|------|------|
| Rack Coordinates: | Local Rack Coordinates: | Local Plate Coordinates: | | | | | | |
| $x_{rc} :=$ | $x_r := x_{rc} - 21$ | $x_p :=$ | | | | | | |
| j | 1 | j | | | | | | |
| <table border="1" style="display: inline-table;"><tr><td>24.15</td></tr><tr><td>59.80</td></tr><tr><td>45.70</td></tr></table> | 24.15 | 59.80 | 45.70 | $x_r := x_{rc} - 42 - 3.5$ | <table border="1" style="display: inline-table;"><tr><td>0.0</td></tr><tr><td>-4.5</td></tr><tr><td>33.0</td></tr></table> ? | 0.0 | -4.5 | 33.0 |
| 24.15 | | | | | | | | |
| 59.80 | | | | | | | | |
| 45.70 | | | | | | | | |
| 0.0 | | | | | | | | |
| -4.5 | | | | | | | | |
| 33.0 | | | | | | | | |
| | 2 | | | | | | | |
| | $x_r := x_{rc} - 3.8$ according to | | | | | | | |
| | 3 | | | | | | | |
| Total Lift Local Coordinates: | $x_r \cdot W_r + x_p \cdot W_p$ | x_t | | | | | | |
| | j | j | | | | | | |
| | $x_t := \frac{\quad}{W}$ | <table border="1" style="display: inline-table;"><tr><td>2.45</td></tr><tr><td>7.622</td></tr><tr><td>58.256</td></tr></table> | 2.45 | 7.622 | 58.256 | | | |
| 2.45 | | | | | | | | |
| 7.622 | | | | | | | | |
| 58.256 | | | | | | | | |

When $\theta = 0$ let $x := x_t$ $y := x_t$ $z := x_t$
 $\theta = 0.611$ $x := x$ $y := y \cdot \cos[\theta] - z \cdot \sin[\theta]$
 1 1 0 $z := y \cdot \sin[\theta] + z \cdot \cos[\theta]$

Load Point Locations
Local Coordinates:

| | | |
|-----------------------|-------------------|--|
| When $\theta = 0$ let | Side: $X := 10.0$ | Center: $Y := -6.625$ $Z := 37.16$ |
| $\theta = 0.611$ | $X := 10.0$ | $Y := Y \cdot \cos[\theta] - Z \cdot \sin[\theta]$ |
| 1 | 1 | $Z := Y \cdot \sin[\theta] + Z \cdot \cos[\theta]$ |

Reactions at Jack:

| | | | | | | | | | | | | |
|---|---|----------|-------------------------|---|------|------|--|--------|---------|---|--------|--------|
| $J_h := \frac{y \cdot W}{Y \cdot \tan[\phi] - z}$ | J_h | x | y | z | | | | | | | | |
| | i | i | i | i | | | | | | | | |
| | <table border="1" style="display: inline-table;"><tr><td>-393.326</td></tr><tr><td>386.732</td></tr></table> | -393.326 | 386.732 | <table border="1" style="display: inline-table;"><tr><td>2.45</td></tr><tr><td>2.45</td></tr></table> | 2.45 | 2.45 | <table border="1" style="display: inline-table;"><tr><td>7.622</td></tr><tr><td>-27.17</td></tr></table> | 7.622 | -27.17 | <table border="1" style="display: inline-table;"><tr><td>58.256</td></tr><tr><td>52.092</td></tr></table> | 58.256 | 52.092 |
| -393.326 | | | | | | | | | | | | |
| 386.732 | | | | | | | | | | | | |
| 2.45 | | | | | | | | | | | | |
| 2.45 | | | | | | | | | | | | |
| 7.622 | | | | | | | | | | | | |
| -27.17 | | | | | | | | | | | | |
| 58.256 | | | | | | | | | | | | |
| 52.092 | | | | | | | | | | | | |
| $J_v := J_h \cdot \tan[\phi]$ | J_v | X | Y | Z | | | | | | | | |
| | i | i | i | i | | | | | | | | |
| | <table border="1" style="display: inline-table;"><tr><td>-382.493</td></tr><tr><td>1.901 · 10³</td></tr></table> | -382.493 | 1.901 · 10 ³ | <table border="1" style="display: inline-table;"><tr><td>10</td></tr><tr><td>10</td></tr></table> | 10 | 10 | <table border="1" style="display: inline-table;"><tr><td>-6.625</td></tr><tr><td>-26.741</td></tr></table> | -6.625 | -26.741 | <table border="1" style="display: inline-table;"><tr><td>37.16</td></tr><tr><td>26.64</td></tr></table> | 37.16 | 26.64 |
| -382.493 | | | | | | | | | | | | |
| 1.901 · 10 ³ | | | | | | | | | | | | |
| 10 | | | | | | | | | | | | |
| 10 | | | | | | | | | | | | |
| -6.625 | | | | | | | | | | | | |
| -26.741 | | | | | | | | | | | | |
| 37.16 | | | | | | | | | | | | |
| 26.64 | | | | | | | | | | | | |

Vertex = 2
 Wr = 1.75 · 10³

Rack & Plate, 3 Point Suspension
 with Inclined Central Support Jack

page 2

Reactions at Hinges:

$$Pvr_i := \frac{W}{2} \left[1 + \frac{x_i}{X_i} \right] - \frac{Jv_i}{2}$$

$$Pvl_i := Pvr_i - \frac{x_i}{X_i} \cdot W$$

$$Phr_i := -.5 \cdot Jh_i$$

$$Phl_i := -.5 \cdot Jh_i$$

| |
|-------------------------|
| 1.592 · 10 ³ |
| 450.2 |

| |
|-------------------------|
| 1.041 · 10 ³ |
| -101.05 |

| |
|----------|
| 196.663 |
| -193.366 |

FORWARD COMPUTATION

Resolutions of
 Force/Torque
 Sensors:

$$\delta Fz := 1.0 \text{ lbs.}$$

$$\delta Fxy := 0.5 \text{ lbs.}$$

Force Readings with Maximum Errors:

$$Pvr_i := Pvr_i + \delta Fz$$

$$Pvl_i := Pvl_i + \delta Fz$$

$$Phr_i := Phr_i + \delta Fxy$$

$$Phl_i := Phl_i + \delta Fxy$$

Load Point Off-Set Limit:

$$Fz_i := Pvr_i$$

$$Fxy_i := Phr_i$$

$$Zo_i := \frac{2000}{Fxy_i} \left[1 - \frac{Fz_i}{2740} \right]$$

| |
|--------|
| 4.247 |
| -8.662 |

(use minimum absolute value)

Reaction Jack
 Computed:

$$Jh_i := -[Phr_i + Phl_i]$$

| |
|----------|
| -394.326 |
| 385.732 |

$$Jv_i := Jh_i \cdot \tan[\phi_i]$$

| |
|-------------------------|
| -383.465 |
| 1.896 · 10 ³ |

Weight, Computed:

$$Wc_i := Pvr_i + Pvl_i + Jv_i$$

Center of Mass,
 Computed:

$$xc_i := \frac{X_i}{Wc_i} [Pvr_i - Pvl_i]$$

$$yc_i := \frac{Y_i \cdot Jv_i - Z_i \cdot Jh_i}{Wc_i}$$

$$zc_0 := \frac{yc_0 \cdot \cos[\theta_1] - yc_1}{\sin[\theta_1]}$$

$$zc_1 := \frac{yc_0 - yc_1 \cdot \cos[\theta_1]}{\sin[\theta_1]}$$

| |
|-----------------|
| xc _i |
| 2.449 |
| 2.453 |

| |
|-----------------|
| yc _i |
| 7.638 |
| -27.135 |

| |
|-----------------|
| zc _i |
| 58.217 |
| 52.07 |

| |
|-------------------------|
| Wc _i |
| 2.251 · 10 ³ |
| 2.247 · 10 ³ |

Vertex = 2
 3
 Wr = 1.75 · 10

Rack & Plate, 3 Point Suspension
 with Inclined Central Support Jack

page 3

ERROR ESTIMATES

Weight Error:

$$erWr_i := \frac{Wc_i - W}{Wr} \cdot 100$$

$erWr_i$

| |
|--------|
| 0.059 |
| -0.167 |

 % compared with allowable
 .2 %

Center of Mass Error:

$$erx_i := xc_i - x_i$$

erx_i

| |
|--------|
| -0.001 |
| 0.003 |

 compared with allowable
 .4 in.

$$ery_i := yc_i - y_i$$

ery_i

| |
|-------|
| 0.016 |
| 0.035 |

 .4 in.

$$erz_i := zc_i - z_i$$

erz_i

| |
|--------|
| -0.038 |
| -0.022 |

 .4 in.

REFERENCES

- [1] Boeing, U. S. STANDARD EQUIPMENT RACK INTERFACE DEVELOPMENT DOCUMENT, NASA / MSFC, SSP 41090, Draft 6, 6/30/92
- [2] McDonnell - Douglas, ORU HANDLING DEVICE, NASA / KSC, design file No. D0392900, dwg. No. 82K03929, 11/20/92
- [3] McDonnell - Douglas, RACK INSTL / REMOVAL END EFFECTOR ASSY / INSTL, NASA / KSC, design file No. D0393100, dwg. No. 82K03931, 9/30/92